J. Membrane Biol. 67, 13–26 (1982)

The Journal of
Membrane Biology

Rotation of Cells in an Alternating Electric Field: Theory and Experimental Proof

C. Holzapfel, J. Vienken, and U. Zimmermann

Arbeitsgruppe Membranforschung am Institut für Medizin, Kernforschungsanlage Jülich GmbH., Postfach 19 13, 5170 Jülich/BRD (Germany)

Summary. Protoplasts of *Avena sativa* rotate in an alternating electric field provided that at least two cells are located close to each other. An optimum frequency range (20 to 30 kHz) exists where rotation of all cells exposed to the field is observed. Below and above this frequency range, rotation of some cells is only occasionally observed. The angular velocity of rotation depends on the square of the electric field strength. At field strengths above the value leading to electrical breakdown of the cell membrane, rotation is no longer observed due to deterioration of the cells. The absolute value of the angular velocity of rotation at a given field strength depends on the arrangement of the cells in the electric field. A maximum value is obtained if the angle between the field direction and the line connecting the two cells is 45°. With increasing distance between the two cells the rotation speed decreases. Furthermore, if two cells of different radii are positioned close to each other the cell with the smaller radius will rotate with a higher speed than the larger one. Rotation of cells in an alternating electric field is described theoretically by interaction between induced dipoles in adjacent cells. The optimum frequency range for rotation is related to the relaxation of the polarization process in the cell. The quadratic dependence of the angular velocity of rotation on the field strength results from the fact that the torque is the product of the external field and the induced dipole moment which is itself proportional to the external field. The theoretical and experimental results may be relevant for cyclosis (rotational streaming of cytoplasm) in living cells.

Key words cell rotation · polarization · protoplasts · dielectric breakdown

Introduction

Pohl and Crane [22] reported that yeast cells can rotate with a frequency of a few Hz in an alternating electric field in the frequency range between 100 Hz and 500 kHz, but that statistically only a small percentage of the cells in the field will rotate. Pohl [19–21] attributed the rotation of cells to deposition of charges on the cell surface (so-called ambipolar charging) or to the interaction of the external alternating field with intrinsic oscillating dipoles in the cell. Using appropriate experimental conditions Zimmermann et al. [35] recently demonstrated that there exists a narrow optimum frequency range in which nearly all suspended cells exposed to the alternating field will rotate. This optimum frequency range for the rotation of cells varies from one species to another.

Since erythrocyte ghost cells are also able to rotate in an alternating electric field, Zimmermann et al. [35] further concluded that the rotation is attributable to the generation of a dipole by charge separation at the membrane interface and/or orientation of permanent dipoles within the membrane. This assumption is supported by the preliminary finding that artificial lipid vesicles also exhibit rotation phenomena in an alternating electric field *(unpublished data)*.

In this paper we investigate in more detail experimentally and theoretically the dependence of the speed of rotation of mesophyll protoplast cells of *Avena sativa* on the field intensity and on the interaction between adjacent cells of varying size.

Experiments and theory have shown that the rotation of cells can be described by the interaction between electrically induced dipole moments of adjacent cells. The direction and the speed of rotation depend on the relative position of the cells in the external field. As shown theoretically, the optimum frequency range for the occurrence of rotation in the alternating field is determined by the relaxation times of the polarization processes of the cells which result in the generation of dipoles.

The theory suggests that certain properties of the membrane can be deduced from rotational experiments.

Materials and Methods

Rotational experiments were carried out under the light microscope and monitored and recorded for evaluation on a Leitz/Grundig video recording system. The experimental set-up consisted of two parallel platinum electrodes mounted horizontally on a perspex slide and connected to a function generator (Toellner

0022-2631/82/0067-0013 $02.80

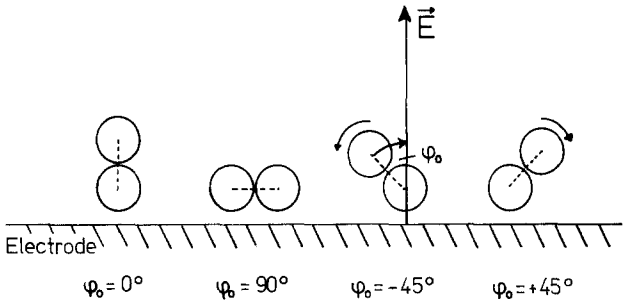

Fig. 1. Illustration of the different relative positions of two cells in the electric field

GmbH, Frankfurt, West Germany, Type TE 7704), which was used as the voltage source for the generation of alternating electric fields [34]. The distance between the electrodes was 300 μm; the temperature was kept at 22 °C. Cell rotation was investigated by applying an alternating voltage of 0.5 to 6 V (sine wave, 20–30 kHz).

Mesophyll cell protoplasts of *Avena sativa* were obtained from leaves by digesting the cell walls enzymatically with cellulysin (Calbiochem, San Diego, Calif.; *see also* [12]).

Protoplasts, suspended in a 0.5 M/liter mannitol solution, were subsequently pipetted between the electrodes and collected by dielectrophoresis (field strength 6.6 kV m^{-1}). For measuring the speed of rotation on the field strength, the cells were allowed to settle down on the microslide. The electric conductivity of the solution was adjusted to be less than 10^{-4} $(\Omega\text{cm})^{-1}$.

Experimental Results

As reported earlier [35], mesophyll protoplasts of *Avena sativa* preferentially rotate in the frequency range of 20 to 30 kHz. Above and below this frequency range only some cells are seen to rotate weakly. The observed angular velocity of rotation is in the order of a few cycles per second.

A prerequisite for the occurrence of rotation is the close proximity of a second cell or some other local disturbance in the field (e.g. due to irregularities of the electrode). Rotation occurs in the plane constituted by the connecting line between the two cells and the electric field vector. The speed and direction of the rotation depend on the relative position of the two cells in the external alternating field. When the two cells are arranged in such a way that their connecting line is parallel to the external field ($\varphi_0 = 0$ in Fig. 1), there is no rotation; nor is there any rotation when the connecting line is vertical with respect to the external field ($\varphi_0 = 90°$). The maximum speed of rotation is observed at $\varphi_0 = \pm 45°$, where φ_0 is the angle between the connecting line between the centers of the two cells and the direction of the external field. If $\varphi_0 = -45°$, rotation is counterclockwise, whereas for $\varphi_0 = +45°$ it is clockwise.

With dielectrophoresis [26] it is possible to collect a large number of cells in the form of pearl chains which are more or less parallel to the external field (Fig. 2). Thus, a large number of "45°-orientations" are established between the cells of neighboring chains, so that the interaction may lead to rotation of many cells in the suspension [35]. Depending on the distances involved, there are both "+45° and −45° orientations"; therefore, clockwise and counterclockwise rotations are statistically distributed in the cell chains.

This phenomenon can be demonstrated particularly well if the alternating voltage is briefly switched off after the cells have arranged themselves into parallel chains. This causes the chains to tilt slightly towards the electrode surfaces because of gravity and Brownian motion. When the alternating voltage is reapplied, the chains can be stabilized in a direction oblique to the field lines by the additional collection of some free cells which bridge the gap between the electrodes. Depending on the angle between these oblique chains and the field direction, the cells within one chain will all rotate in the same direction.

In spite of careful and extensive investigation, rotation of individual cells floating free between the electrodes or allowing to settle down on the microslide was never observed. This observation is in contradiction to reports from Pohl and Crane [22] who state that a single cell is able to rotate. It is not inconceivable that the apparent rotation of "free" cells as described by these authors is due to inaccurate observation. It is extremely difficult to exclude the possibility that other cells are located below or above the focus plane of the "freely" rotating cell under observation. Evidently, such an arrangement of cells can also lead to rotation. In this case the axis of rotation lies in the plane of observation. On the other hand, single cells occasionally rotate when they are close to the electrode surface.

In the range of electric field strength experimentally accessible, the angular velocity of rotation increases with the square of the field strength (14 independent experiments). Typical results are shown in Fig. 3. The dependence of the angular velocity on the square of the field strength is particularly pronounced if the cells are allowed to settle down on the microslide. Otherwise, a certain field strength is required to maintain the cells between the two electrodes. This can lead to the erroneous result that rotation occurs only above a threshold value of the electric field strength *(see below)*.

At higher electric field strengths an upper limit in the external field strength exists above which rotation can no longer be observed. This upper limit arises from the electrical breakdown of the cell membrane [2, 32, 33]. Subsequent release of elec-

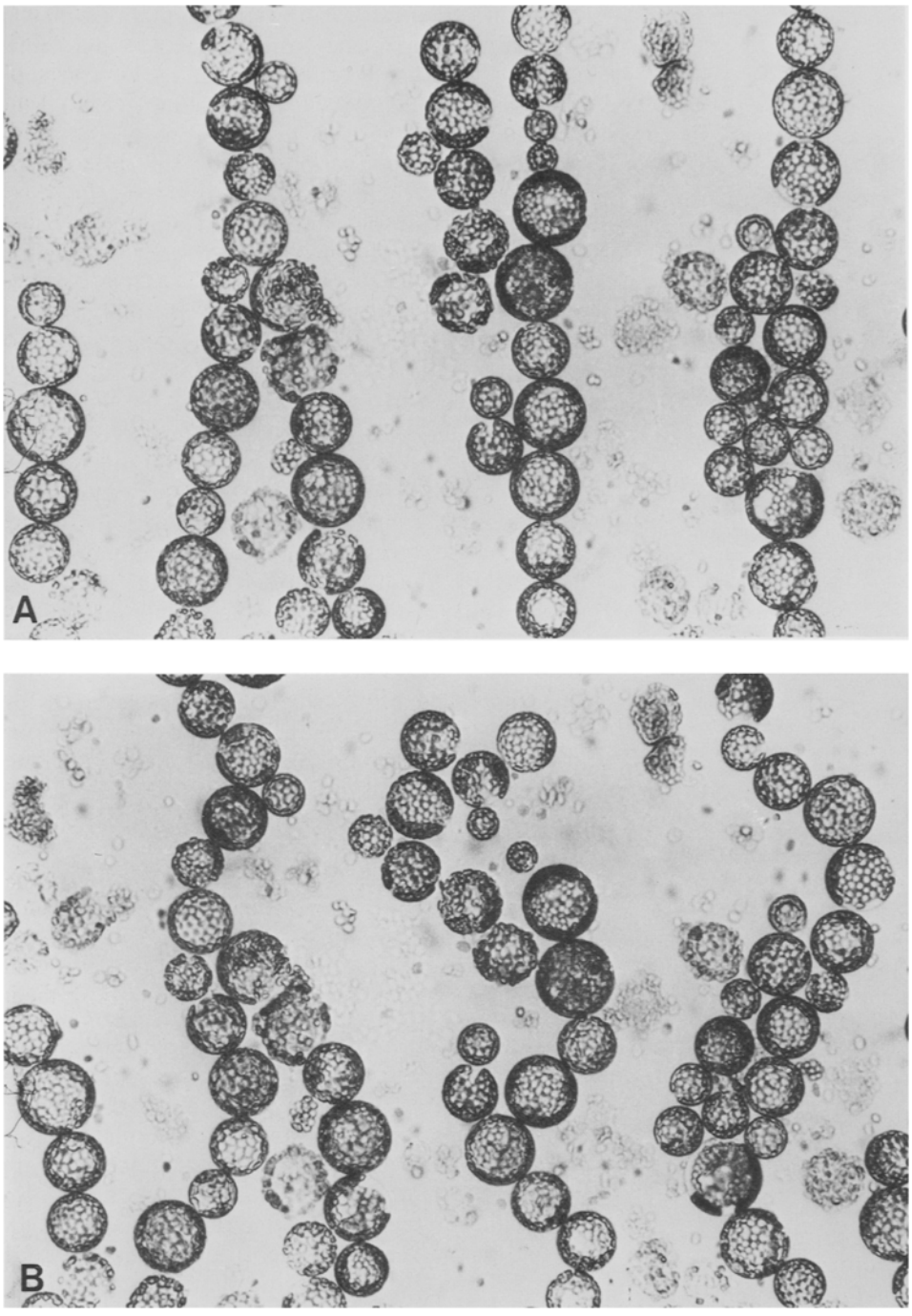

Fig. 2. (*A*): Dielectrophoretic pearl chaining of *Avena sativa* protoplast cells in an alternating electric field ($E = 6.6\,\mathrm{kV\ m^{-1}}$, $\nu = 2\,\mathrm{MHz}$ (200×)). (*B*): Arrangement of *Avena sativa* protoplast cells after switching on the optimum frequency (25 kHz) for rotation ($E = 6.6\,\mathrm{kV\ m^{-1}}$ (200×))

trolyte from the cells and bursting of the cells at higher field strength leads to disturbances and turbulences due to the generation of heat in the solution. At lower frequencies electrical breakdown of the cell membranes is observed at a lower field strength compared with that measured in the optimum frequency range. The frequency dependence of the critical external field strength leading to breakdown of the membranes is expected for two reasons. As shown in Appendix (C) the membrane potential built up across the membrane in response to the external alternating field is a function of frequency, i.e. at lower frequency a higher potential is built up across the membrane for a given field

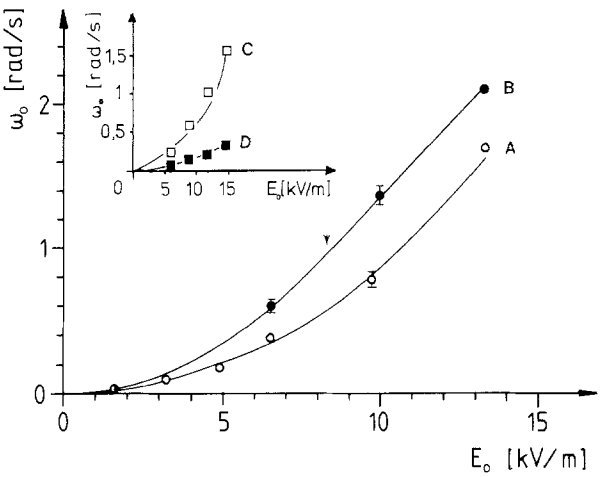

Fig. 3. Dependence of the angular velocity (ω_o) on the field strength (E_o). Pairs of protoplasts of *Avena sativa* (both 18 µm in radius) were investigated at the optimum frequency (25 kHz). The angular velocity is a square function of the field strength (curve *A*). In some experiments the function becomes linear above a certain field strength (for this cell pair $8.3 \pm 0.5\,\mathrm{kV\,m^{-1}}$), indicated by the arrow (curve *B*); for further explanation *see text*. *Inset:* $\omega_o = f(E_0)$ for two cells in close contact with different radii. Curve *C* represents the rotation of the smaller cell ($a = 12.5\,\mu m$); curve *D* represents the rotation of the bigger cell ($a = 18\,\mu m$). Note, that the speed of rotation of the smaller cell is higher than that of the bigger one. Each point represents the average of four measurements. The standard deviation is shown when it is larger than the symbols. The curves represent least-square fits

strength. Thus, the critical membrane potential is reached at lower values of the external field strength. Furthermore, as shown by Zimmermann and Benz for cell membranes [5, 31] and for artificial lipid bilayer membranes [3, 4], the breakdown voltage itself depends on the frequency (i.e. on the pulse length). With decreasing frequency the breakdown voltage decreases in a certain frequency range by a factor of 2 and more (from about 1 to 0.4 V, if only a single membrane is considered). Thus, it is extremely difficult to measure accurately the dependence of the angular velocity of rotation on the field strength below the optimum frequency of the alternating field. Above the optimum frequency range, rotation is only occasionally observed (*see* section called "Theoretical Interpretation..." for explanation).

A further interesting finding of these studies is that at any given field intensity the rotation speed also depends on the ratio of diameters of neighboring cells. At a "45°-orientation" of a large and a small cell, the small cell rotates considerably faster than the larger cell (*see inset*, Fig. 3).

In a parallel set of experiments a 1% glutardialdehyde solution was pipetted carefully onto the cells between the two electrodes during rotation. 10 min after fixation, rotation of the cells is still observed at the same frequency. However, after about 30 min, the optimum frequency range for rotation is occasionally shifted to a value of about 2 MHz and higher. This shift in frequency, which may result from the changes in the electric membrane properties by fixation, explains the previously described observation that cells which were fixed by glutardialdehyde for a longer time showed no rotation phenomenon [35]. The maximum frequency obtained from the frequency generator is 2 MHz. Thus as pointed out earlier [35], it is not possible to detect rotation beyond this limiting frequency with this equipment.

That the cells are indeed fixed by glutardialdehyde 5 min after application is indicated by the finding that the cells can be exposed to much higher external electric field strengths than untreated cells. Higher field strengths are required for rotation as well. Due to cross-linking of the membrane components by glutardialdehyde treatment, the breakdown voltage of all biological membranes so far investigated is shifted to very high values [30, 33]. It was not possible accurately to determine the frequency dependence of rotation of the fixed cells on the electric field strength because the cells were slightly deformed after fixation and sticking between adjacent cells after dielectrophoretic collection was greatly increased. Cell adhesion obviously hindered rotation.

Theoretical Interpretation of the Experimental Results

The experimental results presented here can be interpreted theoretically by assuming that the rotation in the alternating electric field arises from the interaction of electrically induced dipole moments in adjacent cells. In other words, we postulate that a cell can only rotate by its interaction with another adjacent cell or by its proximity to a local disturbance in the field. Geometric irregularities and/or the locally varying composition of the electrode material can also lead to the same time-dependent dipole moments in an alternating field and are thus equivalent to the presence of another cell. This dipole moment then interacts with the dipole moment of a cell in the vicinity and makes it rotate.

In a constant external field $\vec{E}_o$ a dipole $\vec{M}$ is generated in the cell which is orientated parallel or antiparallel to the external field lines [Eq. (A5)]

$$\vec{M} = \beta \cdot \vec{E}_o. \tag{1}$$

The parameter β represents the polarizability of the cell. For a spherical cell surrounded by a noncon-

ducting membrane the following equation holds [Eq. (A8)]

$$\beta = -2\pi\varepsilon_o a^3 \tag{2}$$

where a is the radius of the cell and $\varepsilon_o = 8.854 \cdot 10^{-12}\,\mathrm{Fm}^{-1}$ is the permittivity of the free space.

The generation of the dipole requires a certain time which is given by the relaxation time τ of the processes leading to polarization. In an alternating electric field the dipole strength thus varies with time and is dependent on the angular frequency ω of the field $\vec{E}(t)$ [Eq. (A14)]

$$\vec{M}(t) = \frac{\beta}{\tau} \int_{-\infty}^{t} \vec{E}(\vartheta)\, e^{-\frac{t-\vartheta}{\tau}}\, d\vartheta. \tag{3}$$

Thus, for a single cell exposed to an alternating field $\vec{E}(t) = \vec{E}_o \cdot \cos(\omega t)$ the dipole is given by

$$\vec{M}(t) = \frac{\beta}{1+(\omega\tau)^2} \cdot \vec{E}_o(\cos\omega t + \omega\tau \cdot \sin\omega t). \tag{4}$$

ω is defined by $\omega = 2\pi\nu$, where ν is the frequency and ω the angular frequency.

Equation (4) demonstrates that the largest dipole moment occurs at $\omega = 0$, i.e. in a constant field. With increasing frequency the dipole moment decreases. Simultaneously as given by the second term in the bracket an increasing phase shift is observed between the external field and the dipole moment; i.e. the generation of the dipole is delayed with respect to the external field. At very high frequencies, i.e. when $\omega\tau \gg 1$, the time during one phase of the external field is not sufficient for the generation of a dipole. In consequence, the dipole moment tends towards zero, while the phase shift tends towards $-\pi/2$.

If there are two adjacent cells present in an alternating external electric field, then the field of the dipole of the second cell also contributes to the generation of the dipole in the first cell and vice versa, in addition to the influence exerted by the external field. The electric field arising from a dipole $\vec{M}$ in its environment is given by [Eq. (A4)]

$$\vec{E}_m = -\frac{1}{4\pi\varepsilon_o}\left\{\frac{\vec{M}}{r^3} - 3(\vec{M}\vec{r})\frac{\vec{r}}{r^5}\right\} \tag{5}$$

with the vector $\vec{r}$ which connects the two cell centers (Fig. 4). The total field which is responsible for the generation of a dipole in a given cell is given by the sum of the alternating external field and the dipole field of the second cell which varies with time [Eq. (A18)]

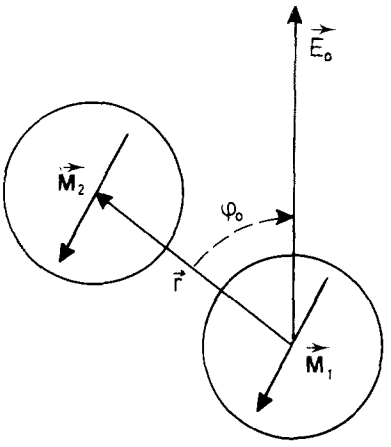

Fig. 4. Illustration of the vectors $\vec{M}_1$, $\vec{M}_2$, and $\vec{r}$ and of the angle φ_o for two spherical cells in the external field $\vec{E}_o$

$$\vec{E}_2 = \vec{E}(t) - \frac{1}{4\pi\varepsilon_o}\left\{\frac{\vec{M}_2(t)}{r^3} - 3(\vec{M}_2(t)\vec{r})\frac{\vec{r}}{r^5}\right\}. \tag{6}$$

In response to this time-dependent total field the dipole $\vec{M}_1$ of the first cell is generated [Eq. (A19)]

$$\vec{M}_1(t) = \frac{\beta}{\tau} \int_{-\infty}^{t} \vec{E}_2(\vartheta)\, e^{-\frac{t-\vartheta}{\tau}}\, d\vartheta \tag{7}$$

with the time ϑ as an integration variable.

An analogous set of equations is valid for the first cell and for the dipole of the second cell, whereby the subscripts 1 and 2 have to be exchanged (*see* Appendix A).

This system of equations describes the time dependence of the two dipole moments $\vec{M}_1$ and $\vec{M}_2$ of the two cells in an alternating external field $\vec{E}(t)$. The integration of this system of equations is given in Appendix A.

Figure 5 shows the dependence of the amplitude of the dipole moment and the phase shift in relation to the external electric field on the frequency of the alternating field, calculated from Eqs. (A41, A39, A40). Analogous to the case of one single cell, the dipole moments of the two cells decrease with increasing frequency, while the phase shifts increase.

Due to the time varying field strength and direction of the total field and due to the delayed generation of the dipoles, no equilibrium state can be established. Thus, a torque is exerted on each of the two cells (Appendix B)

$$\vec{N}_2 = \vec{M}_2 \wedge \vec{E} - \frac{1}{4\pi\varepsilon_o}\vec{M}_2 \wedge \mathrm{grad}\left(\frac{\vec{M}_1\vec{r}}{r^3}\right). \tag{8}$$

An analogous equation applies to the torque exerted on the other cell.

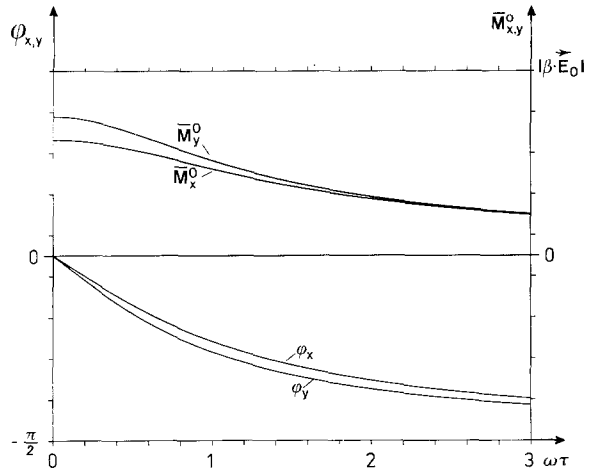

Fig. 5. Calculated dependence of the amplitude $\bar{M}_0$ of the dipole vector and of the phase angles φ_x and φ_y on the frequency of the external alternating field according to Eqs. (A41), (A39) and (A40), respectively

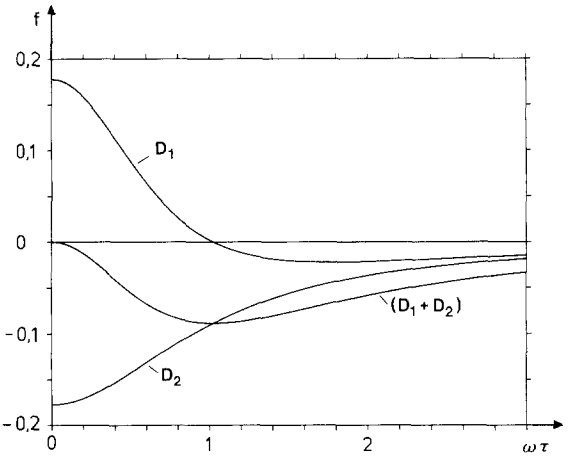

Fig. 6. Calculated variation of the averaged torque (function f) and its two parts with the frequency of the external field according to Eq. (B7) for the case $\tau_1=\tau_2=\tau$, $a_1=a_2=a$, $r=a_1+a_2=2a$. D_1 ... dipole-field interaction, D_2 ... dipole-dipole interaction

The two terms, i.e. the torque on the dipole $\vec{M}_2$ in the external field and the torque in the field of the other dipole $\vec{M}_1$ are dependent on time. However, the total torque $\vec{N}_2$ is constant with time and is non-zero; thus the time average of this total torque does not vanish resulting in rotation of the cell. The solution of the system of Eqs. (6) and (7) and the time-averaging of the torque in Eq. (8) leads to a mean torque [Eq. (B7)]:

$$\langle \vec{N}_2 \rangle = \tfrac{1}{2}\beta \cdot \vec{E}_o^2 \cdot \sin\varphi_o \cdot \cos\varphi_o \cdot f \tag{9}$$

in the presence of an alternating field $\vec{E}(t) = \vec{E}_0 \cdot \cos(\omega t)$.

Equation (9) explains the experimentally determined dependence of the rotation on the relative position of the two cells in the external field. For $\varphi_o = 0$ and $\varphi_o = 90°$ the torque vanishes, while for $\varphi_o = 45°$ it is at its maximum.

The function f is dependent on the radii of the cells, on the relaxation times of the polarization processes of the cells, on the angular frequency ω of the external field and on the distance r between the two cells (*see* Appendix B). The mean torque $\langle \vec{N} \rangle$, and the function f, respectively, are composed of two terms, analogous to the torque in Eq. (8) [Eq. (B8)],

$$f = D_1 + D_2. \tag{10}$$

These are the torque of the dipole in the external field ($\sim D_1$) and the torque of the dipole in the field of the second dipole ($\sim D_2$). Figure 6 shows the dependence of these two terms and the sum f on $\omega\tau$. When $\omega\tau = 0$, i.e. in a constant field, both terms are equal and opposite because the dipoles are generated in the equilibrium state; therefore, the sum of the torques vanishes.

With increasing frequency the absolute values of the two terms decrease, because the strength of the dipoles diminishes. With increasing frequency the orientation will be determined predominantly by the external field, because the contribution of the fields of the dipoles to the total field becomes weaker; thus, the dipoles become less aligned with increasing frequency. Therefore, the torque of the dipole in the external field ($\sim D_1$) decreases more rapidly than that arising from the interaction between the dipoles ($\sim D_2$). The total mean torque, the sum of these two terms, achieves a maximum at $\omega\tau = 1$. At very high frequencies, i.e. for $\omega\tau \gg 1$, the dipoles and, in turn, the torque tends to zero. Consequently, no rotation can occur. This dependence of the torque on frequency explains the experimental observation that rotation predominantly occurs in a certain narrow frequency range. From the frequency correlated with the maximum torque it is possible to estimate the relaxation time $\tau = 1/\omega$ of the polarization processes. With $\nu = 25$ kHz, τ is calculated to be about 6 µsec for the membranes of protoplast cells of *Avena sativa*.

Assuming that the dipole is generated by charge separation at the membrane, and not by phospholipid orientation, the relaxation time is given by Eq. (A17) in [13]. With 1 µF/cm^2 for the specific capacity, 10 µm for the radius, and 10^{-4} $(\Omega\,\mathrm{cm})^{-1}$ for the external conductivity, the time constant is calculated to be 5 µsec, which is in good agreement with the result from rotational experiments.

The field-dipole interaction drives the ions forming the dipole of the cell according to the torque

calculated in Eqs. (8) or (9). The movement of the ions is transferred to the whole cell by collision and momentum transfer between the ions surrounded by a hydration shell and the neutral particles of the solution in the cell. This is expressed by the Boltzmann equation for each single species of particle in the conducting fluid. Averaging the Boltzmann equation with the appropriate distribution function of the molecular velocities yields the momentum equation for the conducting fluid. This describes the influence of the electric field on the bulk fluid. At collisional equilibrium which is established after a time very much shorter than one cycle of the applied external electric field the torque acting on the charged particles also acts on the total fluid.

In order to calculate the speed of rotation, one has to take into account the frictional forces acting on the cells. At a constant angular velocity of rotation ω_o of the cell the torque $\langle \vec{N} \rangle$ is balanced by the opposite directed torque arising from the frictional forces [6]

$$\vec{N}_f = -8\pi\eta\omega_o a^3 \tag{11}$$

where a is the radius of the rotating cell and η is the viscosity of the surrounding medium. The equilibrium condition is given by

$$\langle \vec{N} \rangle + \vec{N}_f = 0. \tag{12}$$

Combining Eqs. (9)–(12) yields the angular velocity of rotation

$$\omega_o = -\frac{\varepsilon_o}{8\eta} \cdot \vec{E}_o^2 \cdot \sin\varphi_o \cdot \cos\varphi_o \cdot f. \tag{13}$$

For calculation of ω_o, the function f must be known.

The dependence of the function f on the radii a_1 and a_2 of the two interacting cells is reduced to a dependence on the ratio a_1/a_2 if the distance between the two cell centers becomes $r = a_1 + a_2$, i.e. if the cells are just touching each other. Thus, for cells with equal diameters, which are just in contact at their external membrane surfaces, the speed of rotation is not dependent on the radius. Cells with different radii, on the other hand, exhibit varying speeds of rotation. Figure 7*a* shows the dependence of the function f for cell of different size. It is evident that a large cell will rotate more slowly near a small cell ($a_2 > a_1$) than vice versa ($a_2 < a_1$). This theoretical prediction is corroborated by experimental evidence. As expected, the function f depends on the distance between the cells if $r > a_1 + a_2$, i.e. if the cells no longer touch each other. Figure 7*b* shows

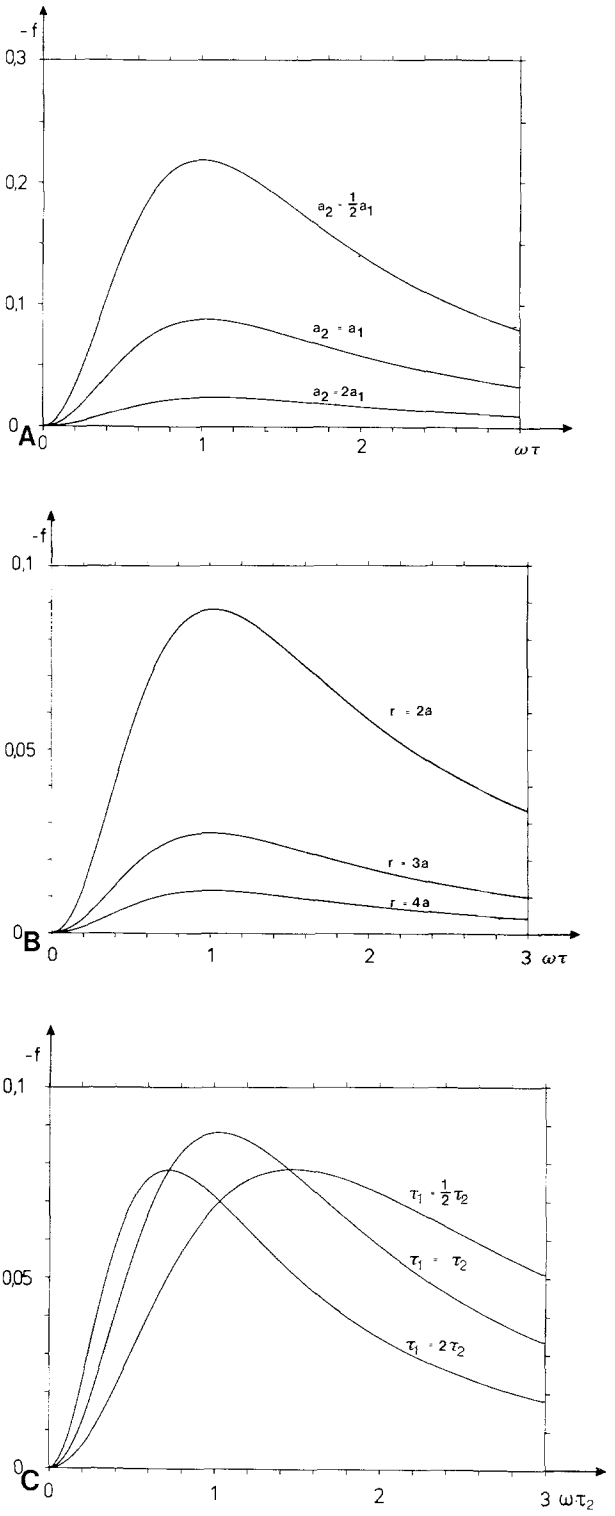

Fig. 7. (**a**): Dependence of the function f on the frequency of the external alternating field for different radii a_1 and a_2 of two interacting cells calculated from Eq. (B8), ($\tau_1 = \tau_2 = \tau$, $r = a_1 = a_2$). (**b**): Dependence of the function f on the frequency of the external alternating field for different distances between two interacting cells calculated from Eq. (B8), ($\tau_1 = \tau_2 = \tau$, $a_1 = a_2 = a$). (**c**): Dependence of the function f on the frequency of the external alternating field for different relaxation times of the two interacting cells calculated from Eq. (B8), ($a_1 = a_2$, $r = a_1 + a_2$)

the decrease of f over the entire frequency range with ever increasing distance between the cells, which is due to the reduction in the dipole-dipole interaction.

The function f is also dependent on the relaxation times τ_1 and τ_2 for the polarization processes of the cells. If the relaxation times of the two cells are equal ($\tau_1=\tau_2=\tau$) the maximum of the function f occurs at $\omega\tau=1$ *(see above)*. Different relaxation times lead to a reduction of the function f and to a shift of the maximum. Figure 7*c* demonstrates that the maximum is shifted towards higher frequencies when the relaxation time of the rotating cell τ_2 is longer than the relaxation time τ_1 of the other cell. The maximum occurs at $\omega\tau_2>1$. Conversely, the maximum occurs at lower frequencies ($\omega\tau_2<1$), if $\tau_2<\tau_1$.

So far it has not been possible to provide unequivocal evidence for this theoretical prediction. Zimmermann et al. [35] reported that in a mixed cell suspension consisting of Friend cells and yeast cells each of the species exhibits maximum rotation at the same frequencies found for Friend and yeast cells alone, i.e. 25 and 180 kHz, respectively. No shift in the optimum frequency for rotation could be detected. The reason for this may be that the resolution of the experimental set-up is not sufficiently high for the detection of small frequency shifts.

At the frequency at which rotation occurs, the pearl-chains have an orientation of about 45° relative to the direction of the external field (Fig. 2*b*). This may be caused by superposition of the potentials of the dipole in the external field and in the field of the adjacent dipole.

There is still a discrepancy between the theoretical value of the angular velocity of the spinning cell and the experimental value. The observed rotation speed is higher than theoretically predicted because of an underestimation of the electrostatic forces. The interaction between the two dipoles is calculated using the field strength of the dipole of one cell at the center of the second cell, i.e. assuming a uniform field of one dipole throughout the area of the second cell. In fact we have to take into account that the field is not uniform. If the cells are close together the attractive force between the surface charge of one cell and the adjacent opposite surface charge of the second cell is much higher than the force calculated from the dipole interaction assuming the dipoles are in the center of the cells. So far the theory developed in this paper is a first-order approximation.

Most important, the theory predicts the experimentally measured quadratic dependence of the angular velocity ω_o on the field intensity $\vec{E}_o$.

Discussion

The qualitative agreement of the theory with the experimental results strongly supports the view that the rotation of cells in an alternating electric field is caused by the interaction between induced dipoles generated in adjacent cells.

The rotation of cells requires that at least two cells arranged as described above are present in the field and that they are positioned close to each other. Thus, it seems very unlikely that a single cell far away from the electrodes and from other cells in the suspension could rotate as claimed by Pohl and Crane [22]. The occurrence of an optimum frequency range, in which all cells in a suspension exposed to the alternating field rotate, is also predicted by the theory.

The strongest evidence for the theory is the experimental finding that the rotation speed increases with the square of the electric field strength, especially at small field strength values. The theory predicts a quadratic dependence of the angular velocity of the rotating cell on the field strength. This is a result of the torque being a product of two factors both of which depend linearily on the field strength [Eq. (B1)].

At higher field strength values, however, we occasionally find experimentally a more linear relationship between the angular velocity and the field strength (ref. Fig. 3). We believe that this is caused by hydrodynamic interaction between the rotating cells.

Especially at higher angular velocities the cells do not rotate freely in the sense of the boundary conditions used to calculate the frictional force [6]. The hydrodynamic boundary layer around the rotating cell is disturbed by the other cells. The frictional force between the rotating cell and the surrounding fluid is proportional to the angular velocity of the cell. Similarly, the frictional force of a disturbing cell in the moving fluid is also proportional to the velocity of the fluid relative to the disturbing cell. Therefore, we have a momentum transfer between the two cells via hydrodynamic interaction which is approximately proportional to the square of the angular velocity of the rotating cell. Inserting this into the equilibrium condition [Eq. (12)] yields a linear dependence between the angular velocity of the rotating cell and the electric field.

Thus, a more linear relationship is expected between the angular velocity and the field strength at small distances between the cells and at high field strength where the hydrodynamic interaction is strong whereas the relationship is more quadratic at lower field strength, i.e. where hydrodynamic interac-

tion is weak. This would also explain the data of Mischel and Lamprecht [15] who found a linear relationship between angular velocity and field strength for yeast cells. By extrapolating to zero angular velocity these authors claimed the existence of a threshold value of the electric field below which no rotation occurs.

As shown here, this is not true. A second reason for the erroneous suggestion of a threshold value may arise from experimental conditions used by these authors. Mischel and Lamprecht [15] have probably investigated the rotation phenomenon at a frequency outside of the optimum frequency range, which makes it difficult to induce cell rotation at low field strength. Furthermore, they investigated cells which were held between the electrodes by application of a low field strength, whereas we allowed the cells to settle down on the microslide. The holding field obviously makes it impossible to observe rotation at very low field strengths. Because of the small size of yeast cells budding cells were used by these authors to measure the rotation speed. The buds may considerably increase the frictional forces and, in consequence, as pointed out above, the quadratic relationship between the rotation speed and the field strength would shift to a more linear one. Also the assumption of Mischel and Lamprecht [15] that the rotation of the cells depends on their inertia moment cannot be correct because inertia only influences the angular acceleration and not the steady-state angular velocity of the cells. From the optimum frequency for rotation the relaxation time of the processes resulting in the dipole of a cell can be calculated. The dipole of a cell may be generated either by charge separation at the membrane caused by the movement of the ions in the interior of the cell and in the external space of the cell (interfacial polarization), and/or by dipole orientation within the membrane (dielectric polarization). Depending on the polarization process, the polarizability is given by Eq. (A8) or Eq. (A6).

The dielectric polarization within the membrane is a process very much faster than the interfacial polarization. This is also due to the fact that the membrane capacitance is practically independent of frequency [17, 23, 24]. In the frequency region considered here, the interfacial polarization is superimposed upon dielectric polarization which leads to the rotation of the cells.

The relaxation time depends on the conductivities of the external and internal solutions of the cell and on the conductivity of the membrane [13, 23]. Therefore a shift in the optimum frequency for rotation to higher values which is occasionally observed after treatment of the cells with glutardialdehyde may reflect a slight change in the electric properties of the membrane (*see also* [30]).

We are aware of the fact that the negative value of β in Eq. (2) apparently will not lead to dielectrophoretic collection of the cells. However, the polarization process leading to the dipole of the cell is more complicated than described in this paper. We have only used one relaxation time to describe these processes. In fact there is a phase shift between the charge separation inside the cell and the accumulation of charge at the outside surface of the cell which causes a change in β from positive to negative value during the entire process [18]. Also the nonuniformity of the external field is changed due to charge movement in the alternating field. This is also depending on the geometric arrangement of the electrodes. With two parallel cylindric wires between two parallel glass plates the charge movement in even pure water will change the field gradient. In the first moment the field will increase towards the wires (vacuum field). Concomittant with movement of ions in the medium between the electrodes the field will change. Near the cylindric wire the field will be weaker than in the center between the electrodes. The relaxation time for this process is of the same order as the relaxation time for the polarization of the cells. Therefore also a negative value of β will lead to dielectrophoretic collection of the cells at the electrodes, since the gradient of the field points away from the electrodes. The interference of these processes may also be the reason that the optimum frequency range for rotation differs from the optimum frequency range for dielectrophoretic collection of the cells.

A third process resulting in a cell dipole is the movement of counter-charges close to the charged membrane surface. This process is very slow and should be important only in the frequency region up to about 1 kHz [17, 25].

Experiments of cell rotation in an alternating electric field may be a tool in the future to elucidate the main mechanism involved in the generation of the dipole and, in turn, of other appropriate membrane parameters.

Finally we would like to point out that the results reported here may have relevance for the explanation of cyclosis (rotational streaming and rotation of organelles in plant cells and slime moulds [1, 9, 11, 14, 16, 27–29]). In the light of our results it seems possible that electric field effects are involved in the generation of cyclosis, although the origin of the electric field required is not clear. However, it is conceivable that oscillating carrier systems in the membrane leads to an alternating field required for electric field-mediated movement.

We are grateful to Dr. Schwan, University of Pennsylvania, for critical and stimulating discussion. We also thank H. Wolters for expert technical assistance, H. Jaeckel for growing the plants, and S. Alexowsky for typing this manuscript.

This work was supported by a grant from the Deutsche Forschungsgemeinschaft, Sonderforschungsbereich 160 (to U.Z.).

Appendix

A. *Generation of Dipoles in Adjacent Cells in an Alternating Electric Field*

We consider a spherical cell with an electrically conductive interior and a nonconducting membrane separating the interior from a conductive external medium. Exposure of the cell to an electric field $\vec{E}_o$ leads to the generation of a dipole in the cell. The dipole field is superposed on the external field $\vec{E}_o$. The total field is described by the Laplace's equation for the potential Φ in the charge free space

$$\text{div grad}\,\Phi = 0 \tag{A1}$$

with

$$\vec{E} = -\,\text{grad}\,\Phi \tag{A2}$$

together with the appropriate boundary conditions [7, 10].

The potential can be expanded into a series of Legendre polynomials. The charge distribution on the surface of the sphere can be described by a dipole $\vec{M}$ located in the center of the sphere, i.e. the potential is described by the first and the second term of the expansion

$$\Phi = -\vec{E}_o\vec{r} + \frac{1}{4\pi\varepsilon_o}\frac{(\vec{M}\vec{r})}{r^3} \tag{A3}$$

where $\vec{r}$ is the radius vector from the center of the sphere to the point considered.

The total field at distance $r = |\vec{r}|$ from the center of the cell is

$$\vec{E} = \vec{E}_o - \frac{1}{4\pi\varepsilon_o}\,\text{grad}\left(\frac{\vec{M}\vec{r}}{r^3}\right) = \vec{E}_o - \frac{1}{4\pi\varepsilon_o}\left\{\frac{\vec{M}}{r^3} - 3(\vec{M}\vec{r})\cdot\frac{\vec{r}}{r^5}\right\}. \tag{A4}$$

The dipole of the cell is generated in a direction parallel or antiparallel to the external field $\vec{E}_o$

$$\vec{M} = \beta\cdot\vec{E}_o. \tag{A5}$$

For a dielectric sphere of radius a the Laplace equation yields the polarizability

$$\beta = 4\pi\varepsilon_o a^3\cdot\left(\frac{\varepsilon-1}{\varepsilon+2}\right) \tag{A6}$$

where $\varepsilon = \varepsilon_i/\varepsilon_e$ is the ratio of the dielectric constants ε_i of the sphere to ε_e of the surrounding medium.

On the other hand for a conducting sphere of conductivity σ_i surrounded by a medium of conductivity σ_e the polarizability is

$$\beta = 4\pi\varepsilon_o a^3\cdot\left(\frac{\sigma_i-\sigma_e}{\sigma_i+2\cdot\sigma_e}\right). \tag{A7}$$

A cell surrounded by a nonconducting membrane is electrically equivalent to a nonconducting sphere. Therefore with $\sigma_i = 0$ the polarizability according to Eq. (A7) is given by

$$\beta = -2\pi\varepsilon_o a^3. \tag{A8}$$

The generation of the dipole does not occur instantaneously. The relaxation time depends on the process leading to polarization. The generation of the dipoles is assumed to be a first-order reaction, i.e. the change of the dipole moment with time is proportional to the difference between the momentary and the steady-state value,

$$\frac{d}{dt}\vec{M} = \frac{1}{\tau}(\beta\cdot\vec{E}_o - \vec{M}). \tag{A9}$$

Applying a constant field $\vec{E}_o$ at time $t=0$, the solution of Eq. (A9) is given by

$$\vec{M}(t) = \beta\cdot(1-e^{-t/\tau})\cdot\vec{E}_0. \tag{A10}$$

On removal of the field the decay of the dipole due to relaxation of the charge distribution is given by

$$\vec{M}(t) = \vec{M}_o\cdot e^{-t/\tau}. \tag{A11}$$

In a variable external field $\vec{E}(t)$ a variable dipole $\vec{M}(t)$ is generated. In this case $\vec{M}(t)$ is the superposition of the momentary generated dipole and all the previously generated dipoles which are decaying exponentially.

At the time ϑ a dipole is generated during the time interval $d\vartheta$

$$d\vec{M}(\vartheta) = \frac{\beta}{\tau}\vec{E}(\vartheta)\,d\vartheta. \tag{A12}$$

Later, at time t, this dipole has decayed to

$$d\vec{M}(t) = d\vec{M}(\vartheta)\cdot e^{-\frac{t-\vartheta}{\tau}}. \tag{A13}$$

Thus the total dipole at time t is the vector sum (*see also* [8])

$$\vec{M}(t) = \int_{-\infty}^{t} d\vec{M}(t) = \frac{\beta}{\tau}\int_{-\infty}^{t}\vec{E}(\vartheta)\,e^{-\frac{t-\vartheta}{\tau}}\,d\vartheta. \tag{A14}$$

The lower time limit of the integral was set to $-\infty$ in order to avoid transient processes which also decay with the time constant τ.

We now consider two cells placed in an external field

$$\vec{E}(t) = \vec{E}_o\cdot e^{i\omega t}. \tag{A15}$$

φ_o is the angle between the field direction and the line connecting the two centers (Fig. 4).

In each of the cells a dipole $\vec{M}_1$ and $\vec{M}_2$, respectively, is generated.

The total field $\vec{E}_1(t)$ at the second dipole $\vec{M}_2$ is the sum of the external field $\vec{E}(t)$ and the field of the dipole $\vec{M}_1$

$$\vec{E}_1(t) = \vec{E}_o e^{i\omega t} - \frac{1}{4\pi\varepsilon_o}\left\{\frac{\vec{M}_1(t)}{r^3} - 3(\vec{M}_1(t)\vec{r})\frac{\vec{r}}{r^5}\right\}. \tag{A16}$$

This field generates the second dipole

$$\vec{M}_2(t) = \frac{\beta_2}{\tau_2}\int_{-\infty}^{t}\vec{E}_1(\vartheta)\cdot e^{-\frac{t-\vartheta}{\tau_2}}\,d\vartheta. \tag{A17}$$

By analogy we have the field $\vec{E}_2(t)$ at the first dipole $\vec{M}_1$ where

$$\vec{E}_2(t)=\vec{E}_o e^{i\omega t}-\frac{1}{4\pi\varepsilon_o}\left\{\frac{\vec{M}_2(t)}{r^3}-3(\vec{M}_2(t)\vec{r})\frac{\vec{r}}{r^5}\right\} \tag{A18}$$

and

$$\vec{M}_1(t)=\frac{\beta_1}{\tau_1}\int_{-\infty}^{t} E_2(\vartheta)\,e^{-\frac{t-\vartheta}{\tau_1}}d\vartheta. \tag{A19}$$

In Eq. (A18) we use the same vector $\vec{r}$ as in Eq. (A16) because making the substitution $\vec{r}'=-\vec{r}$, we obtain the same sign for the second term in the brackets. The system of Eqs. (A16)-(A19) describes the time dependence of the two dipoles in the external alternating field.

Differentiation of the two Eqs. (A17) and (A19) yields the differential equation for the dipoles $\vec{M}_1$ and $\vec{M}_2$ analogously to Eq. (A9). Scalar multiplication with the radius vector $\vec{r}$ yields the system of differential equations

$$\dot{\vec{y}}+A_1\cdot\vec{y}=\vec{f}_1(t) \tag{A20}$$

for the components

$$\vec{y}=\begin{pmatrix}(\vec{M}_1\vec{r})\\(\vec{M}_2\vec{r})\end{pmatrix} \tag{A21}$$

of the dipoles $\vec{M}_1$ and $\vec{M}_2$.

The matrix is given by

$$A_1=(A_{kl}^{(1)})=\begin{pmatrix}\frac{1}{\tau_1} & \frac{-\beta_1}{2\pi\varepsilon_o\tau_1 r^3}\\ \frac{-\beta_2}{2\pi\varepsilon_o\tau_2 r^3} & \frac{1}{\tau_2}\end{pmatrix} \tag{A22}$$

and the perturbation vector by

$$\vec{f}_1(t)=\begin{pmatrix}\frac{\beta_1}{\tau_1}\\ \frac{\beta_2}{\tau_2}\end{pmatrix}\cdot(\vec{E}_o\vec{r})\cdot e^{i\omega t}. \tag{A23}$$

Vector multiplication with $\vec{r}$ from the right side of Eqs. (A17) and (A19) yields the system of differential equations

$$\dot{\vec{x}}+A_2\cdot\vec{x}=\vec{f}_2(t) \tag{A24}$$

for the other two components

$$\vec{x}=\begin{pmatrix}(\vec{M}_1\wedge\vec{r})\\(\vec{M}_2\wedge\vec{r})\end{pmatrix} \tag{A25}$$

of the dipoles. In this case, the matrix is given by

$$A_2=(A_{kl}^{(2)})=\begin{pmatrix}\frac{1}{\tau_1} & \frac{\beta_1}{4\pi\varepsilon_o\tau_1 r^3}\\ \frac{\beta_2}{4\pi\varepsilon_o\tau_2 r^3} & \frac{1}{\tau_2}\end{pmatrix} \tag{A26}$$

and the perturbation vector by

$$\vec{f}_2(t)=\begin{pmatrix}\frac{\beta_1}{\tau_1}\\ \frac{\beta_2}{\tau_2}\end{pmatrix}\cdot(\vec{E}_o\wedge\vec{r})\cdot e^{i\omega t}. \tag{A27}$$

The solution of this system for $t\gg\tau$, i.e. after the decay of initial transient processes yields

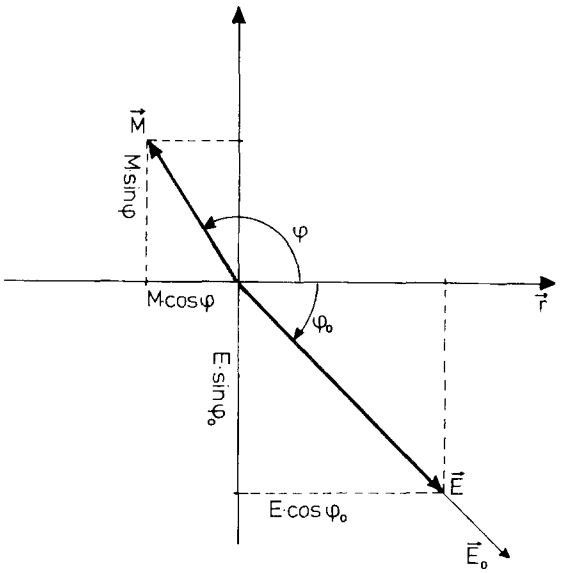

Fig. 8. Diagrammatic representation of the position of the two vectors $\vec{M}$ and $\vec{E}$ at a certain time (t_1 in Fig. 9)

$$(K_{kl})=\begin{pmatrix}(\vec{M}_1\vec{r}) & (\vec{M}_2\vec{r})\\ (\vec{M}_1\wedge\vec{r}) & (\vec{M}_2\wedge\vec{r})\end{pmatrix} \tag{A28}$$

where

$$K_{kl}=\frac{G_{kl}\cdot e^{i\omega t}}{C_k-\omega^2+i\omega B} \tag{A29}$$

$$B=Trace\,(A_1)=Trace\,(A_2)=\frac{1}{\tau_1}+\frac{1}{\tau_2} \tag{A30}$$

$$C_k=Det\,(A_k). \tag{A31}$$

For $k=1$ we have

$$C_1=\frac{1}{\tau_1\cdot\tau_2}\cdot\left(1-\frac{\beta_1\cdot\beta_2}{(2\pi\varepsilon_o r^3)^2}\right) \tag{A32}$$

and for $k=2$ we have

$$C_2=\frac{1}{\tau_1\cdot\tau_2}\cdot\left(1-\frac{\beta_1\cdot\beta_2}{(4\pi\varepsilon_o r^3)^2}\right). \tag{A33}$$

The quantities G_{kl} are defined by

$$\begin{aligned}
G_{11}&=\frac{\beta_1}{\tau_1}\cdot(\vec{E}_o\vec{r})\cdot(i\omega+A_{22}^{(1)}-A_{21}^{(1)})\\
G_{12}&=\frac{\beta_2}{\tau_2}\cdot(\vec{E}_o\vec{r})\cdot(i\omega+A_{11}^{(1)}-A_{12}^{(1)})\\
G_{21}&=\frac{\beta_1}{\tau_1}\cdot(\vec{E}_o\wedge\vec{r})\cdot(i\omega+A_{22}^{(2)}-A_{21}^{(2)})\\
G_{22}&=\frac{\beta_2}{\tau_2}\cdot(\vec{E}_o\wedge\vec{r})\cdot(i\omega+A_{11}^{(2)}-A_{12}^{(2)}).
\end{aligned} \tag{A34}$$

From these we obtain the real parts needed for the calculation of the torque

$$\begin{aligned}
Re(K_{kl})=&\frac{1}{(C_k-\omega^2)^2+(\omega B)^2}\cdot\\
&\cdot\{[Re(G_{kl})\cdot(C_k-\omega^2)+Im(G_{kl})\cdot\omega\cdot B]\cdot\cos\omega t\\
&-[Im(G_{kl})\cdot(C_k-\omega^2)-Re(G_{kl})\cdot\omega\cdot B]\cdot\sin\omega t\}.
\end{aligned} \tag{A35}$$

Fig. 8 shows one of the dipole vectors and the external field.

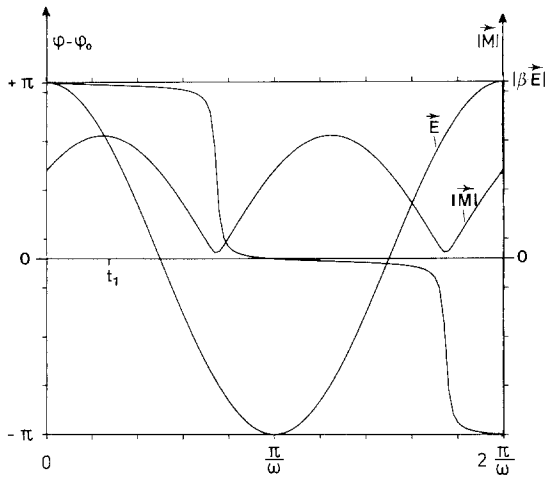

Fig. 9. Time dependence of the dipole vector $\vec{M}$ calculated from Eq. (A36). The absolute value of the vector and the angle between $\vec{M}$ and the external field vector $\vec{E}_o$ are shown for the case $\omega\tau=1$, $\tau_1=\tau_2=\tau$

The components of the vectors are given by

$$M_1\cdot\cos\varphi=\frac{1}{r}Re(K_{11}) \quad M_2\cdot\cos\varphi=\frac{1}{r}Re(K_{12})$$
$$M_1\cdot\sin\varphi=\frac{1}{r}Re(K_{21}) \quad M_2\cdot\sin\varphi=\frac{1}{r}Re(K_{22}) \tag{A36}$$

and

$$E\cdot\cos\varphi_o=\frac{1}{r}(\vec{E}\vec{r}) \quad E\cdot\sin\varphi_o=\frac{1}{r}(\vec{E}\wedge\vec{r}) \tag{A37}$$

in the cartesian coordinate system in which the radius vector lies in the x-axis.

Figure 9 shows the delay between the external field and the generation of the dipole $\vec{M}$. This is also represented by a phase shift between the two vectors. Each of the components of the vector $\vec{M}$ has its own phase shift relative to the external field.

Using the complex vector

$$\vec{M}=\vec{M}_o e^{i\omega t} \tag{A38}$$

with the components

$$\vec{M}_o=\begin{pmatrix}M_x^o\\M_y^o\end{pmatrix}=\frac{1}{r}\cdot\begin{pmatrix}(\vec{M}_o\vec{r})\\(\vec{M}_o\wedge\vec{r})\end{pmatrix}=\begin{pmatrix}\overline{M}_x^o\cdot e^{i\varphi_x}\\\overline{M}_y^o\cdot e^{i\varphi_y}\end{pmatrix}$$

we obtain the phase angles φ_x and φ_y of the two components

$$\text{tang}\,\varphi_x=\frac{Im(M_x^o)}{Re(M_x^o)}=\frac{Im(K_{11}(t=0))}{Re(K_{11}(t=0))} \tag{A39}$$

and

$$\text{tang}\,\varphi_y=\frac{Im(M_y^o)}{Re(M_y^o)}=\frac{Im(K_{21}(t=0))}{Re(K_{21}(t=0))}. \tag{A40}$$

The amplitude is given by

$$\overline{\vec{M}}_o=\begin{pmatrix}\overline{M}_x^o\\\overline{M}_y^o\end{pmatrix}=\frac{1}{r}\begin{pmatrix}\{(Re(K_{11}(t=0)))^2+(Im(K_{11}(t=0)))^2\}^{\frac{1}{2}}\\\{(Re(K_{21}(t=0)))^2+(Im(K_{21}(t=0)))^2\}^{\frac{1}{2}}\end{pmatrix} \tag{A41}$$

and the absolute value of the real part of the vector

$$Re(\vec{M})=\begin{pmatrix}Re(M_x)\\Re(M_y)\end{pmatrix} \tag{A42}$$

is given by

$$|\vec{M}|=\{(Re(M_x))^2+(Re(M_y))^2\}^{\frac{1}{2}}$$
$$=\frac{1}{r}\{(Re(K_{11}))^2+(Re(K_{21}))^2\}^{\frac{1}{2}}. \tag{A43}$$

The absolute value of the dipole vector in Fig. 9 is time dependent whereas the amplitude is time independent.

Figure 5 shows the dependence of the amplitude $\overline{\vec{M}}_o$ of the dipole vector and of the phase angles φ_x and φ_y on the frequency of the external alternating field $\vec{E}(t)$.

B. *Interaction Between the Dipoles and the External Alternating Field*

The torque which acts on the dipole $\vec{M}_2$ in the electric field $\vec{E}_1$ is given by

$$\vec{N}_2=\vec{M}_2\wedge\vec{E}_1 \tag{B1}$$

where only the real parts of the vectors are used. Since all the vectors lie in one plane we can use the identities

$$\vec{M}_2\wedge\vec{E}_o=\frac{1}{r^2}\{(\vec{M}_2\wedge\vec{r})\cdot(\vec{E}_o\vec{r})-(\vec{M}_2\vec{r})\cdot(\vec{E}_o\wedge\vec{r})\} \tag{B2}$$

and

$$\vec{M}_2\wedge\vec{M}_1=\frac{1}{r^2}\{(\vec{M}_2\wedge\vec{r})\cdot(\vec{M}_1\vec{r})-(\vec{M}_2\vec{r})\cdot(\vec{M}_1\wedge\vec{r})\}. \tag{B3}$$

With the identity

$$e^{i\omega t}=\cos\omega t+i\cdot\sin\omega t \tag{B4}$$

and with field $\vec{E}_1(t)$ from Eq. (A16) we obtain for the torque

$$\vec{N}_2=\frac{1}{r^2}\{(\vec{M}_2\wedge\vec{r})\cdot(\vec{E}_o\vec{r})\cos\omega t-(\vec{M}_2\vec{r})\cdot(\vec{E}_o\wedge\vec{r})\cos\omega t\}$$
$$+\frac{1}{4\pi\varepsilon_o r^5}\{(\vec{M}_2\vec{r})\cdot(\vec{M}_1\wedge\vec{r})+2\cdot(\vec{M}_1\vec{r})\cdot(\vec{M}_2\wedge\vec{r})\}. \tag{B5}$$

An analogous equation is obtained for the torque $\vec{N}_1$ which acts on the dipole $\vec{M}_1$ in the field $\vec{E}_2$.

The two parts of the torque $\vec{N}_2$ are both time dependent with the frequency ν identical to the frequency of the external field $\vec{E}(t)$. However, the torque $\vec{N}_2$, i.e. the sum of the two parts in Eq. (B5) is time independent and nonzero. Therefore the time average of the torque is also nonzero leading to the rotation of the cell. It is possible to eliminate the sin- and cos-functions in Eq. (B5) by averaging over time. Given the identities

$$\langle\cos^2\omega t\rangle=\langle\sin^2\omega t\rangle=\tfrac{1}{2} \tag{B6}$$

and

$$\langle\cos\omega t\cdot\sin\omega t\rangle=0$$

and given the equations for the components of $\vec{M}_1$, $\vec{M}_2$, and $\vec{E}_o$ the time-averaged torque yields

$$\langle \vec{N}_2 \rangle = \tfrac{1}{2}\beta_2 \cdot \vec{E}_o^2 \cdot \sin\varphi_o \cdot \cos\varphi_o \cdot f(\beta_1\beta_2\tau_1\tau_2 a_1 a_2 \omega r). \tag{B7}$$

According to Eq. (B5) the function f consists of two terms. The first term describes the torque which acts on the dipole $\vec{M}_2$ due to the external field $\vec{E}_o$. The second term describes the torque acting on $\vec{M}_2$ due to the field of the other dipole $\vec{M}_1$.

The function f in Eq. (B7) is explicitely given by

$$f = \frac{1}{\tau_2}[S_1 + S_2] = D_1 + D_2 \tag{B8}$$

where

$$S_1 = \frac{Q_2}{R_2} - \frac{Q_1}{R_1}$$

$$S_2 = \frac{\beta_1}{\tau_1} \cdot \frac{1}{R_1 \cdot R_2} \cdot \frac{1}{4\pi\varepsilon_o r^3}(Q_3 + 2 \cdot Q_4)$$

$$Q_1 = \left(A_{11}^{(1)} - \frac{\beta_1}{\tau_1}\frac{\tau_2}{\beta_2}A_{21}^{(1)}\right) \cdot (C_1 - \omega^2) + \omega^2 B$$

$$Q_2 = \left(A_{11}^{(2)} - \frac{\beta_1}{\tau_1} \cdot \frac{\tau_2}{\beta_2}A_{21}^{(2)}\right) \cdot (C_2 - \omega^2) + \omega^2 B$$

$$R_1 = (C_1 - \omega^2)^2 + (\omega B)^2$$

$$R_2 = (C_2 - \omega^2)^2 + (\omega B)^2$$

$$Q_3 = P_1 \cdot P_2 + P_3 \cdot P_4$$

$$Q_4 = P_5 \cdot P_6 + P_7 \cdot P_8$$

$$P_1 = \left(A_{11}^{(1)} - \frac{\beta_1}{\tau_1} \cdot \frac{\tau_2}{\beta_2} \cdot A_{21}^{(1)}\right) \cdot (C_1 - \omega^2) + \omega^2 B$$

$$P_2 = \left(A_{22}^{(2)} - \frac{\beta_2}{\tau_2} \cdot \frac{\tau_1}{\beta_1} \cdot A_{12}^{(2)}\right) \cdot (C_2 - \omega^2) + \omega^2 B$$

$$P_3 = \omega \cdot \left[C_1 - \omega^2 - B \cdot \left(A_{11}^{(1)} - \frac{\beta_1}{\tau_1} \cdot \frac{\tau_2}{\beta_2} \cdot A_{21}^{(1)}\right)\right]$$

$$P_4 = \omega \cdot \left[C_2 - \omega^2 - B \cdot \left(A_{22}^{(2)} - \frac{\beta_2}{\tau_2} \cdot \frac{\tau_1}{\beta_1} \cdot A_{12}^{(2)}\right)\right]$$

$$P_5 = \left(A_{22}^{(1)} - \frac{\beta_2}{\tau_2} \cdot \frac{\tau_1}{\beta_1} \cdot A_{12}^{(1)}\right) \cdot (C_1 - \omega^2) + \omega^2 B$$

$$P_6 = \left(A_{11}^{(2)} - \frac{\beta_1}{\tau_1} \cdot \frac{\tau_2}{\beta_2} \cdot A_{21}^{(2)}\right) \cdot (C_2 - \omega^2) + \omega^2 B$$

$$P_7 = \omega \cdot \left[C_1 - \omega^2 - B \cdot \left(A_{22}^{(1)} - \frac{\beta_2}{\tau_2} \cdot \frac{\tau_1}{\beta_1} \cdot A_{12}^{(1)}\right)\right]$$

$$P_8 = \omega \cdot \left[C_2 - \omega^2 - B \cdot \left(A_{11}^{(2)} - \frac{\beta_1}{\tau_1} \cdot \frac{\tau_2}{\beta_2} \cdot A_{21}^{(2)}\right)\right].$$

The matrix components $A_{kl}^{(m)}$ are given by Eqs. (A22) and (A26) and the coefficients B and C_k are given by Eqs. (A30)-(A33).

Figure 10 shows the time dependent parts of the torque $\vec{N}_2$ according to Eq. (B5) for the case $\omega\tau = 1$. Because of the phase shift between the external field $\vec{E}(t)$ and the dipole moment $\vec{M}_2(t)$ the part of the torque due to the interaction between $\vec{M}_2$ and $\vec{E}$ alternates between negative and positive values. There is no phase shift between the two dipole moments; and their interaction, which is described by the second part of Eq. (B5), gives only negative values. The total torque, i.e. the sum of both parts, is independent of time and shows a negative value which is equal to the time averaged value $\langle \vec{N}_2 \rangle$. Figure 6 illustrates the dependency of the two parts of the averaged torque $\langle \vec{N}_2 \rangle$ on the frequency ν of the external field $\vec{E}(t)$ according to Eq. (B7).

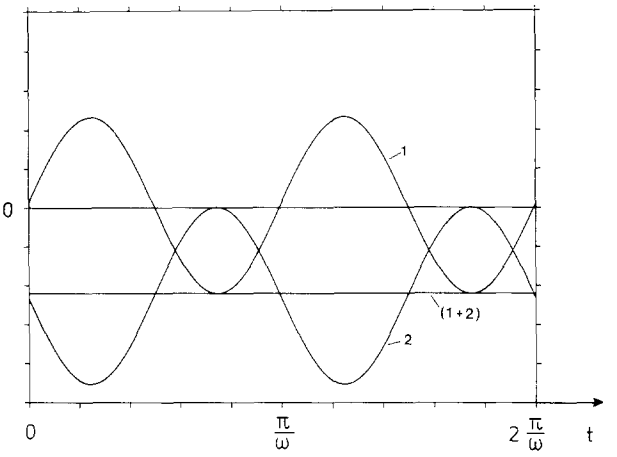

Fig. 10. Time dependence of the individual parts of the torque for the case $\omega\tau = 1$, ($\tau_1 = \tau_2 = \tau$), calculated from Eq. (B5). The upper curve (1) is the part of the torque due to the interaction between the dipole $\vec{M}_2$ and the external field $\vec{E}$. The lower curve (2) is the part of the torque due to the interaction between the two dipoles $\vec{M}_1$ and $\vec{M}_2$. The total torque $\vec{N}_2$ is the sum (1+2) of both

C. *Time Dependence of the Induced Membrane Potential*

The field strength and the potential in the external space around a spherical cell are described by Eqs. (A3) and (A4). The field inside the cell is

$$\vec{E}_i = \vec{E}_o + \alpha \cdot \vec{M}(t). \tag{C1}$$

If the dipole reaches steady state the field inside the cell vanishes, i.e.

$$\vec{E}_i = 0 \quad \text{if } \vec{M} = -2\pi\varepsilon_0 a^3 \vec{E}_o. \tag{C2}$$

Substituting Eq. (C2) into Eq. (C1) yields

$$\alpha = \frac{1}{2\pi\varepsilon_o a^3}. \tag{C3}$$

Thus, the potential inside the cell is given by

$$\Phi_i = -(\vec{E}_o \vec{r}) - \frac{(\vec{M}\vec{r})}{2\pi\varepsilon_o a^3}. \tag{C4}$$

The time dependent membrane potential is given by the difference of the potentials outside and inside the cell

$$U_m(t) = \Phi_e - \Phi_i \quad \text{where } |\vec{r}| = a. \tag{C5}$$

This yields the relationship between the time-dependent membrane potential $U_m(t)$ induced by interfacial polarization at the membrane and the corresponding dipole

$$U_m(t) = \frac{3}{4\pi\varepsilon_o a^3}(\vec{M}(t)\,\vec{a}) \tag{C6}$$

where $\vec{a}$ is the radius vector from the center of the spherical cell to the surface, i.e. $|\vec{a}| = a$.

For the simple case of a single cell in an alternating field $\vec{E} = \vec{E}_o \cdot \cos\omega t$, Eq. (A14) yields

$$\vec{M}(t) = -\frac{2\pi\varepsilon_o a^3}{1+(\omega\tau)^2} \cdot \vec{E}_o \cdot (\cos\omega t + \omega\tau \cdot \sin\omega t) \quad \text{(C7)}$$

for the dipole and for the membrane potential

$$U_m(t) = \frac{3}{2} \frac{(\vec{E}_0(\vec{a})}{1+(\omega\tau)^2} \cdot (\cos\omega t + \omega\tau \cdot \sin\omega t) \quad \text{(C8)}$$

with the amplitude

$$U_m^o = \frac{1.5(\vec{E}_o \cdot \vec{a})}{\sqrt{1+(\omega\tau)^2}}.$$

On the other hand, for a constant field applied to the cell at time $t=0$ we get for the dipole

$$\vec{M}(t) = -2\pi\varepsilon_o a^3 \cdot (1-e^{-t/\tau}) \cdot \vec{E}_o \quad \text{(C9)}$$

and for the membrane potential

$$U_m(t) = -\tfrac{3}{2} \cdot (1-e^{-t/\tau}) \cdot E_0 \cdot a \cdot \cos\vartheta \quad \text{(C10)}$$

in agreement with Jeltsch and Zimmermann [13]. ϑ is the angle between the field direction and the radius vector $\vec{a}$.

References

1. Allen, N.S., Allen, R.D. 1978. Cytoplasmic streaming in green plants. *Annu. Rev. Biophys. Bioeng.* **7**:497–526
2. Benz, R., Beckers, F., Zimmermann, U. 1979. Reversible electrical breakdown of lipid bilayer membranes: A charge-pulse relaxation study. *J. Membrane Biol.* **48**:181–204
3. Benz, R., Zimmermann, U. 1980. Pulse-length dependence of the electrical breakdown in lipid bilayer membranes. *Biochim. Biophys. Acta* **597**:637–642
4. Benz, R., Zimmermann, U. 1980. Relaxation studies on cell membranes and lipid bilayers in the high electric field range. *Bioelectrochem. Bioenerg.* **7**:723–739
5. Benz, R., Zimmermann, U. 1981. High electric field effects on the membrane of *Halicystis parvula*. *Planta* **152**:314–318
6. Berker, R. 1963. Intégration des équations du mouvement d'un fluide visqueux incompressible. *In:* Handbuch der Physik VIII/2. S. Flügge and C. Truesdell, editors. pp. 1–384. Springer-Verlag, Berlin-Göttingen-Heidelberg
7. Böttcher, C.J.F. 1973. Theory of Electric Polarization. Vol. I: Dielectrics in Static Fields. Elsevier, Amsterdam-London-New York
8. Böttcher, C.J.F., Bordewijk, P. 1978. Theory of Electric Polarization. Vol. II: Dielectrics in Time-Dependent Fields. Elsevier, Amsterdam-Oxford-New York
9. Cobbold, P.H. 1980. Cytoplasmic free calcium and amoeboid movement. *Nature (London)* **285**:441–446
10. Cole, K.S. 1968. Membranes, Ions and Impulses. University of California Press, Berkeley, Los Angeles
11. Forde, J., Steer, M.W. 1976. Cytoplasmic streaming in *Elodea*. *Can. J. Bot.* **54**:2688–2694
12. Hampp, R., Ziegler, H. 1980. On the use of *Avena* protoplasts to study chloroplast development. *Planta* **147**:485–494
13. Jeltsch, E., Zimmermann, U. 1979. Particles in a homogeneous electrical field: A model for the electrical breakdown of living cells in a Coulter Counter. *Bioelectrochem. Bioenerg.* **6**:349–384
14. Kamiya, N. 1959. Protoplasmic streaming. *Protoplasmatologia* **8**:3a
15. Mischel, M., Lamprecht, I. 1980. Dielectrophoretic rotation in budding yeast cells. *Z. Naturforsch.* **35c**:1111–1113
16. O'Brien, T.P., McCulley, M.E. 1970. Cytoplasmic fibres associated with streaming and saltatory-particle movement in *Heracleum mantegazzianum*. *Planta (Berlin)* **94**:91–94
17. Pethig, R. 1979. Dielectric and Electronic Properties of Biological Materials. John Wiley & Sons. Chichester-New York-Brisbane-Toronto
18. Pohl, H.A. 1978. Dielectrophoresis. Cambridge University Press, Cambridge-London-New York-Melbourne
19. Pohl, H.A. 1979. Do cells in the reproductive state exhibit a Fermi-Pasta-Ulam-Fröhlich resonance and emit electromagnetic radiation? *Research Note* **98**, Oklahoma State University
20. Pohl, H.A. 1980. Natural electrical *rf*-oscillation from cells. *Research Note* **111**, Oklahoma State University
21. Pohl, H.A. 1981. Biological dielectrophoresis. *In:* Electric Field Effects in Biological Membranes. U. Zimmermann and R. Benz, editors. Springer-Verlag, Berlin-Heidelberg-New York *(in press)*
22. Pohl, H.A., Crane, J.S. 1971. Dielectrophoresis of cells. *Biophys. J.* **11**:711–727
23. Schwan, H.P. 1957. Electrical properties of tissue and cell suspensions. *In:* Advances in Biological and Medicine Physics. J.H. Lawrence and C.A. Tobias, editors. pp. 147–209. Academic Press Inc., New York
24. Schwan, H.P. 1963. Determination of biological impedances. *In:* Physical Techniques in Biological Research. W.L. Nastuk, editor. Vol. VI, pp. 323–407. Academic Press, New York and London
25. Schwarz, G. 1962. A theory of the low-frequency dielectric dispersion of colloidal particles in electrolyte solution. *J. Phys. Chem.* **66**:2636–2642
26. Schwarz, G., Saito, M., Schwan, H.P. 1965. On the orientation of nonspherical particles in an alternating electrical field. *J. Chem. Phys.* **43**:3562–3569
27. Simons, P.J. 1981. The role of electricity in plant movements. *New Phytol.* **87**:11–37
28. Tazawa, M., Kikuyama, M., Shimmen, T. 1976. Electric characteristics and cytoplasmic streaming of *Characeae* cells lacking tonoplast. *Cell Struct. Funct.* **1**:165–176
29. Tazawa, M., Kishimoto, U. 1968. Cessation of cytoplasmic streaming of *Chara* internodes during action potential. *Plant Cell Physiol.* Tokyo **9**:361–368
30. Zimmermann, U., Beckers, F., Coster, H.G.L. 1977. The effect of pressure on the electrical breakdown in the membranes of *Valonia utricularis*. *Biochim. Biophys. Acta* **464**:399–416
31. Zimmermann, U., Benz, R. 1980. Dependence of the electrical breakdown voltage on the charging time in *Valonia utricularis*. *J. Membrane Biol.* **53**:33–43
32. Zimmermann, U., Groves, M., Schnabl, H., Pilwat, G. 1980. Development of a new Coulter Counter system: Measurement of the volume, internal conductivity, and dielectric breakdown voltage of a single guard cell protoplast of *Vicia faba*. *J. Membrane Biol.* **52**:37–50
33. Zimmermann, U., Pilwat, G., Beckers, F., Riemann, F. 1976. Effects of external electrical fields on cell membranes. *Bioelectrochem. Bioenerg.* **3**:58–83
34. Zimmermann, U., Scheurich, P. 1981. High frequency fusion of plant protoplasts by electric fields. *Planta* **151**:26–32
35. Zimmermann, U., Vienken, J., Pilwat, G. 1981. Rotation of cells in an alternating electric field: The occurrence of a resonance frequency. *Z. Naturforsch.* **36c**:173–177

Received 19 May 1981; revised 3 September, 17 November 1981